Ma 14: Solid State Laser Principles II

1. Abstract

The process of *l*ight *a*mplification by *s*timulated *e*mission of *r*adiation (laser) can currently provide electromagnetic radiation with exceptional properties from the infrared over the full visible to the ultraviolet spectral range and in special cases into the x-ray regime. It is particularly the coherence in the phase and direction of laser emission that has allowed for its wide spread usage in industrial, medical and scientific applications, largely surpassing the capabilities of any other light source. Lasers currently allow for the highest precision in the measurement of frequency and time to be achieved, with a relative accuracy in the range of and even below $\Delta\nu/\nu = 10^{-15}$. This is in competition with and can surpass the cesium clock standard based on microwave technology. The directionality of laser emission has allowed for long distance measurements on the order of tens to a hundred kilometers in monitoring atmospheric distortions for ground based telescopes in astronomy or in determining constituents of the mesosphere in environmental applications. Even distances of hundreds of thousands of kilometers have been measured by determining the distance to the moon with a precision of a few centimeters. On smaller length scales, resolution far below the wavelength of light can be achieved on the order of tens of nanometers in the imaging of macromolecular systems and organelles of cells in biology. The relative motion of atoms in molecules can be observed with a precession on the order of tens of picometers with the temporal resolution offered by femtosecond laser pulses and the recent development of attosecond technology offers the resolution of electron dynamics. With respect to power, the continuous wave power of standard lasers extends into the kilowatt range and a peak power up to the Petawatt domain can be achieved with special pulsed lasers. This allows for standard applications such as high accuracy material machining for medical and industrial applications and provides an easy access to nonlinear optics. On the upper end of this power scale, even the regime of relativistic optics can be explored. This short summary is only a selected list out of much a larger catalogue of capabilities and applications of laser technology that are rooted in the unique coherence of this radiation source. This catalogue is continuously expanding and it provides the motivation to understand the fundamental principles underlying laser technology.

2. Preparation

2.1 Fundamental Principles of the Laser (review of Ba14)

While there are different mechanisms for obtaining the coherent emission of light from a medium, light amplification by stimulated emission of radiation or *lasing* is most commonly realized by **pumping** an **active medium** within a **cavity** or **optical resonator**. These three fundamental elements of a laser are employed to obtain a particular set of conditions for the interaction of an optical medium with the light quanta or **photons** of a radiation field. The function behind these three elements becomes clear when considering the type of processes that can take place in the interaction of light with a medium, the probability of these processes and the conditions that are necessary for enhancing one particular type of event. In view of the black body radiation reported by Wilhelm Wien and its interpretation by Max Planck at the turn of the last century, Albert Einstein was able to formulate the equilibrium state of a

quantized radiation field with its source and derive the three basic processes of **absorption**, **spontaneous emission** and **stimulated emission** together with the respective probabilities described by the **Einstein coefficients** B_{nm}, A_{mn} and B_{mn}. Among these three processes, it is only stimulated emission that generates photons or electromagnetic radiation fully equivalent in **frequency**, **phase**, **polarization** and **direction** in the amplification of light. These properties are responsible for the distinctive coherent emission of a laser. Due to this, the elements of a laser are configured to particularly enhance stimulated emission in its competition with absorption and spontaneous emission. These work against coherent amplification by annihilating photons or generating incoherent radiation.

In order to enhance the probability of stimulated emission over an absorption process, the active medium usually provides a **three** or **four level structure** of quantized states that are coupled in a particular manner via **radiative** and **non-radiative** processes (see Fig. 1). The pumping process serves to deposit energy into the active medium, which populates the excited energy levels and brings the system into the state **population inversion** between the two levels that serve for the **lasing transition**. When the population of an excited state level exceeds the population in the energetically lower level, the probability of stimulated emission surpassed the respective rate of absorption. Pumping an active medium for a continuous, steady-state cycling through the three or four levels of the system and indirectly populating the state involved in the stimulated emission process is commonly achieved by **optical pumping** (flash or arc lamps, diodes or other lasers). Alternatively, pumping can also be achieved without radiation through electric discharge (*i.e.* HeNe, Ar^+, and N_2 laser). Coherent emission can also be obtained from other processes such as the luminescence of chemical reactions (*i.e.* HCl laser) or be induced by the acceleration of electrons in their passage through magnetic fields of alternating polarity (wigglers in a free electron laser).

Further considering the competition between spontaneous and stimulated emission, the medium is commonly brought into an optical resonator, which consists of reflective faces that trap the emission in specific modes. The dimensions of the cavity determine the frequencies at which these modes can oscillate. By introducing the resonator, the radiation field is directly coupled back to the active medium. This allows for the number of photons per cavity mode to surpass unity and under these conditions, the probability of stimulated emission exceeds the value for spontaneous emission. For this case, the **threshold for lasing** is meet when the amplification by stimulated emission further compensates the losses within the cavity. When this occurs, the modes of the cavity that are within the bandwidth of the **gain profile** of the medium spontaneously begin to oscillate and the system transfers into the state of lasing. In some cases, the gain of certain laser media is high enough to operate without a cavity (*i.e.* N_2 laser). A **closed cavity** (confinement in all three dimensions) and an **open cavity** (on-axis confinement in one dimension) are principally possible but the exceedingly high number of modes for a reasonable cavity size make closed configurations unpractical for the wavelengths in the ultraviolet, visible and near infrared spectrum. Closed cavities are however used for longer wavelengths in masers (*m*icrowave *a*mplification by *s*timulated *e*mission *r*adiation). Open cavities used for lasers usually consist of two high reflective mirrors, where one of the mirrors shows a slightly lower reflectivity in order to allow for a small percentage of the coherent emission to escape the cavity. The number of nodes along the axis of the resonator defines the **longitudinal modes** of the cavity and their frequencies. While most lasers are designed to operate with a **Gaussian profile** in the cross-section of the intensity distribution normal to the axis of a cavity, the **transversal mode** of an open cavity can

also show nodes (two dimensional **Laguerre-Gaussian** or **Hermite-Gaussian** polynomials for cylindrical or cartesian symmetry, respectively). The structure of the transversal electromagnetic mode (denoted by $\mathbf{TEM_{nm}}$) is determined by the curvature of the cavity mirrors and their distance. These are usually adjusted to meet the **stability criterion**, which describes the capability to contain the radiation within the cavity and avoid losses out of the open configuration. Since the geometry varies for different transversal modes, the frequency of the emission from different modes can be shifted from the frequency of the ideal Gaussian TEM_{00} mode.

2.2 The continuous wave diode and Nd:YAG laser (review of Ba14)

While the active medium of a laser can range form gases to liquids and solutions of dyes, solid-state materials such as crystals or glasses doped with metal ions show many advantages over other media. Next to their specific emission properties, the advantages are generally given by engineering aspects such as their durability, long lifetime, reproducible and stable emission parameters as well as their simple and compact integration into a laser configuration. It is noteworthy, that the first laser realized by Theodore Maiman in 1960 was a solid-state ruby laser (aluminium oxide, Al_2O_3 crystal lattice doped with of Cr^{3+} ions). At the time, the laser was often referred to as an “optical maser” since Charles Townes and Arthur Schawlow obtained the first coherent radiation by stimulated emission in the microwave regime with the ammonia maser in 1954.
Within the class of solid state lasers, the **Nd:YAG** laser (a yttrium aluminium granate, $Y_3Al_5O_{12}$ host crystal doped with Nd^{3+} ions) is one of the most wide spread laser media in industrial and scientific applications. The term scheme for this system is shown in Fig. 1. The system has four discrete absorption bands between the sublevels of the $^4I_{9/2}$ and $^4F_{5/2}$ electronic states of the Nd^{3+} ions in the YAG host lattice between 804.4 and 817.3 nm that are relevant for pumping the system. Non-radiative coupling via **lattice phonons** transfers the system to the sublevels of the $^4F_{5/2}$ state from which lasing transitions to the $^4I_{1/2}$, $^4I_{3/2}$, and $^4I_{9/2}$ sublevels occur at 946, 1064 and 1322 nm, respectively. The cycling through these states constitutes a classical four-level laser medium as shown in Fig. 1. The fast non-radiative relaxation processes together with the long lifetime of the $^4F_{5/2}$ state guarantee high **slope efficiency** and **quantum yield** in the conversion of the pump energy to laser energy output.

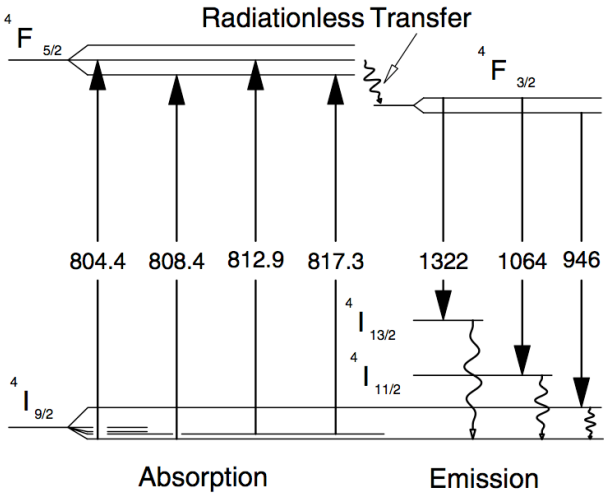

Fig. 1: The term scheme for the Nd:YAG medium with the four-levels relevant for lasing. Taken from [5].

The pumping of the $^4F_{5/2} \leftarrow {}^4I_{9/2}$ transitions in the Nd:YAG medium is generally realized by flash and arc lamps or by diode emission. While flash and arc lamps are economical, their broadband emission is not well matched for pumping the limited spectral range of the narrow absorption bands in the Nd:YAG. This leads to a low efficiency for this arrangement. The tunable emission of a *diode laser* (or arrays of laser diodes for higher power) allows for the pumping of the absorption bands in the Nd:YAG medium at approximately 20 times higher efficiency than with flash or arc lamps. Furthermore, using diode lasers for pumping a Nd:YAG medium results in significantly high stability in the laser emission. It allows for compact integration into the laser arrangement due to the limited size of diodes and avoids the extensive cooling mechanisms associated with the inefficient and instable pumping with flash or arc lamps.
Since diode lasers are becoming an integral part of Nd:YAG laser operation, it is important to review the particular aspects of their function relevant for this application. Generally, diode lasers are **pn-junction semiconductor** lasers, which means they are composed of a p-type and n-type semiconductor materials in mechanical contact. For pumping the Nd:YAG medium, a p- and n-AlGaAs semiconductor material is used with an GaAs **active zone** that spatially separates the charge carriers at the boundary of the heterojunction. This acts as an energy barrier for the **Fermi energy level** before voltage is applied as shown in Fig. 2. Significant differences arise between the working principle of a classical laser configuration and this type of a diode laser arrangement. The emission is obtained from electron-hole recombination when a current is driven through the junction by applying voltage. In this process, excess n-zone electrons at higher energies meet hole charges of the p-zone in the active GaAs region as illustrated in Fig. 2. Radiation from this recombination is obtained at wavelengths that correspond to the energetic separation in the band structure. Amplification is achieved parallel to the junction through a cascade of stimulated emission in the electron-hole recombination at elevated electron densities from the injection current into the active zone through the applied voltage. This cascade of stimulated emission is possible since the band structure is not limited to a discrete energy as the isolated eigenstates of metal ions in a host crystal that follow the **Pauli exclusion principle**. This allows for numerous electrons to occupy a band at varying energies to the point of inversion through the current driven into the active zone.

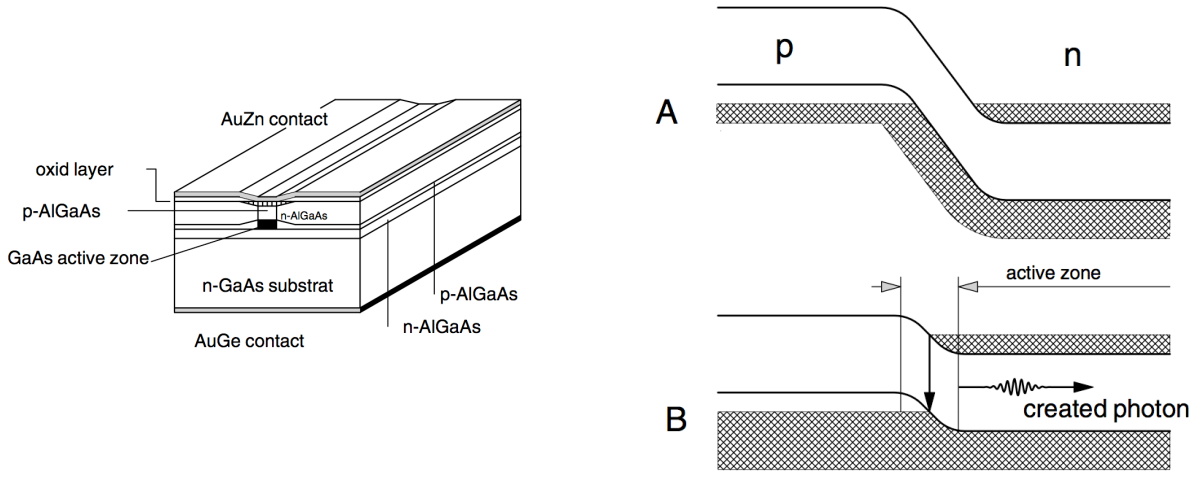

Fig. 2: Schematic of a AlGaAs semiconductor laser (left). Relative energy of the band structure and Fermi level without (A) and with (B) applied voltage as well as the emission from the transition in electron-hole recombination (right). Taken from [5].

Not only the mechanism for obtaining inversion and stimulated emission is changed from a classical lasers arrangement, the guiding of the laser emission in a diode is also fundamentally different. Rather than the free propagation of the coherent radiation within the confinement of the laser cavity, the dimensions of the active zone and the **refractive index** of the materials at the junction act as a **waveguide** in directing the light through the system. Due to this, the laser mode reflects the geometry of the active zone and causes the rectangular like transversal mode profile and high divergence typical for semiconductor lasers. Another important consequence arises form this laser arrangement. The energy of the band structure is dependent on the density of the medium as well as the density of charge carriers in the active zone. This makes the spectrum of the emission obtained from the diode significantly dependent on the temperature and the current in the diode. While the spectral shifting of the emission by temperature and current allows for the practical tunability of laser diode emission, precision temperature and current control is often necessary for stable pumping conditions.

2.3: The Nd:YAG laser with intracavity second harmonic generation and Q-switching

When higher peak power and the respective intensities are desired in the emission or if time resolution is necessary in the application, lasers can easily be transferred into a **pulsed operation**. This is generally realized by **quality-** *i.e.* **Q-switching** (passive or active) or with the technique of **mode locking** (passive or active). Active Q-switching is generally realized with opto-electronic devices such as **Pockels cells** or **opto-acoustic modulators**. When brought into the laser cavity, these devices can periodically alternate in blocking and opening the cavity for the radiation. In a Pockels cells, different polarization states are generated with the modulation of the **bifringence** in crystals such as KTP ($KTiOP_4$ or potassium titanyl phosphate). This is achieved via the **Pockels effect** by bringing the crystal into a strong electric field. The change in polarization of the light can be discriminated with polarizers for opening and closing the cavity. Opto-acoustic modulators utilize radio frequency (rf) piezoelectric transducers that generate standing acoustic waves in crystals such as quartz. This leads to a temporal transmission grating by modulating the refractive index of the crystal and diffracts radiation out of the cavity during the closing period. The *repetition rate* with which laser pulses are emitted can be controlled by the modulation frequency of the Q-switch. The **pulse duration** obtained from Q-switching a cavity is determined by several conditions. It is easily assumed that the duration of the laser pulse is given by the duration that the Q-switch opens the cavity but the degree of population inversion and the rate of its depletion are the essential parameters for the pulse duration. These are dependent on the pump power and duration for which the Q-switch closes the cavity. Furthermore, the **gain bandwidth** sets the lower limit for the pulse duration, which is largely determined by the bandwidth of the emission of the active medium and the cavity arrangement. The relationship of pulse bandwidth and pulse duration is determined by **Fourier transformation**, which gives the **time-bandwidth product** for a particular **envelope function**. The bandwidth $\Delta\nu$ and pulse duration $\Delta\tau$ are usually given at "**full-width at half-maximum**" **(FWHM)** of the profile and for a Gaussian envelope, $\Delta\nu \cdot \Delta\tau = 0.44$.
The Fourier relationship of the frequency and time domain can give a deeper insight to the technique of **mode locking** for realizing pulsed laser emission. **Active mode-locking** is achieved with fast opto-acoustic modulators. For the case of **passive mode-locking**, high intensity radiation in a cavity can self-modulate by nonlinear optical effects such as **Kerr lensing** or **saturable absorbers** and **colliding pulse**

mode-locking can also lead to self-modulation. In order to understand the mechanism of pulse formation, it is instructive to beginning by viewing only a single longitudinal mode at the frequency ν, which is located at the peak of the gain profile. The frequency at which a cavity is periodically opened and closed can be seen as a modulation frequency ν_{mod} of the carrier frequency ν in the longitudinal mode. The modulation of a wave in the time domain with a periodicity significantly longer than the cycle of the wave $\tau_{cyc} < \tau_{mod}$ results by principles of Fourier transformation in the generation of discrete **coherent sidebands** that are positioned in the frequency domain at $\nu \pm \nu_{mod}$. Important to note is the fact that these sidebands are locked in phase with the original carrier frequency. Furthermore, sidebands can also be modulated to further produce frequencies at $\nu \pm n\nu_{mod}$ (n = 1,2,3…). In a continuous wave operation, the longitudinal modes all oscillate independently with a random relative phase to one another. When these modes are modulated, the cascade of sidebands that are generated can coincide in frequency with a neighboring longitudinal mode. The sidebands induce their phase onto the coinciding longitudinal mode and the modes within the gain profil spontaneously lock in phase. This superposition of phase locked longitudinal modes can interfere coherently and lead to highly modulated carrier wave in time. This modulated wave in time can be viewed as a train of pulses that occur at the period that corresponds to the repetition rate with $\tau_{rep} = 1 / \nu_{mod}$. This is equivalent to the round-trip time of light in the cavity. As described by the time-bandwidth product, the duration of the individual pulse structures decrease with an increasing number of modes that are phase locked. This mechanism allows for the coupling of up to 10^6 longitudinal modes in high bandwidth gain media such as Ti:sapphire (sapphire host crystal doped with Ti^{3+}) for laser pulses with a duration down to several femtosecond.

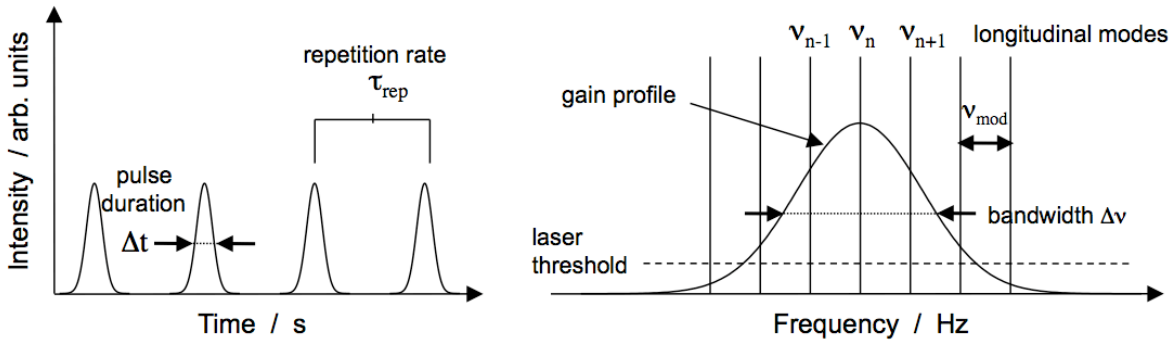

Fig. 3: Schematic for illustrating the principles of mode locking, showing the relationship in the frequency of longitudinal modes, the modulation frequency and the gain bandwidth (right) as well as the respective repetition rate and pulse duration in the time domain (left). Time and frequency domain are related by the time bandwidth product $\Delta\nu \cdot \Delta\tau = 0.44$ for gauss profiles and by $\tau_{rep} = 1 / \nu_{mod}$.

For the Nd:YAG laser, the emission at 1064 nm or ν = 282 THz has a gain bandwidth of $\Delta\nu$ = 0.12 THz, which theoretically translates via the time-bandwidth product to a minimum pulse duration of $\Delta\tau$ = 3.7 ps for a Gaussian envelope. It should be noted that only very sophisticated laser arrangements can approach this pulse duration in a Nd:YAG laser with the shortest pulses reported at about 9 ps. This is due to the difficulties in amplifying the full emission bandwidth or achieving sufficient modulation depths for coupling the necessary modes. Commonly, a slower time scale of the rising and falling edge of pulse is obtained form standard Q-switched Nd:YAG lasers. Here, the rising and falling edge of the pulse are determined by the build-up of lasing after

opening of the Q-switch and the depletion rate of inversion while the Q-switch is open. This can lead to an asymmetric pulse forms. The pulses of Q-switched Nd:YAG lasers can commonly range the nanosecond to the lower microsecond regime. The repetition rates can be adjust by the frequency of the Q-switch and are usually operated in the Hz to kHz range. The **pulse power** and the **peak power** are largely determined by the combination of the repetition rate, the pump power and duration of the pulse.
An important aspect of pulsed lasers is the high field strength and corresponding intensities that can easily be achieved in the emission in this mode. This capability has greatly enhanced the field **nonlinear of optics**. Conversely, the resulting developments in the field of nonlinear optics have allowed for laser technology to advance significantly. A particularly relevant application of nonlinear optics in laser technology is the generation of different frequencies from the laser emission. In many laser applications, specific wavelengths are required and most active media are fixed or limited in the range or bandwidth of their emission. The conversion of a laser frequency via nonlinear processes can be realized in an **intra**- or **extracavity** configuration. In this context, it is advantageous to briefly outline the fundaments of nonlinear processes used for frequency conversion. Generally, nonlinear optical effects are rooted in a displacement of electrons in a dielectric medium or oscillating **polarization** that has a higher order dependency on the amplitude in the electric field of light inducing the effect. This means for the well-known linear effects in optics, the polarization oscillates at the frequency of the inducing electric field of the light. A **nonlinear polarization** can also oscillate at **sum** or **difference frequencies** of the inducing field or fields. Since the higher-order **electric susceptibilities** of most dielectric media are very small, high electric field strengths and the respective intensities are required for inducing a significant nonlinear polarization in a medium.

The general formalism of nonlinear optics can be somewhat complex but the process of frequency doubling in **birefringent**, **non-centrosymetric crystals** is an excellent introduction. It is also one of the most commonly applied nonlinear processes in laser technology. **Frequency doubling** or **second harmonic generation** is an energy and impulse conserving process. Hereby, the energy and impulse of two photons at the fundamental frequency ν are converted to twice the energy of a single photon at the second harmonic frequency 2ν with the respective impulse. While the conservation of energy is easily meet by doubling the frequency, the conservation of the impulse is more complicated. This is due to substantial dispersion of the refractive index in an optically dense medium such as a crystal (see Fig. 4). This leads to the innate shift in the velocity of light generated at double the frequency with respect to the original fundamental wave. In order to meet the **phase-matching conditions** in the velocity of the fundamental frequency and its conversion to its second harmonic in a medium, the different values for the refractive index in the **ordinary** (*o*) and **extraordinary** (*eo*) **axis** of a bifringent crystal are utilized. By placing the optical axis of the crystal at a specific angle to the polarization of the incoming fundamental beam, the effective refractive index for the different frequencies can be compensated according to $n_\nu = n_{2\nu}$. This allows for the conservation of impulse to be realized in matching the phase of the fundamental and second harmonic frequency in their propagation through the crystal. The angle necessary for achieving this situation can be determined from the **refractive index ellipsoid** of a specific material at the position for which the criterion, $n_{2\nu,\,o}(\theta) = n_{\nu\ eo}(\theta)$ is satisfied as shown in Fig. 4. Common materials used for this purpose are BBO (β-barium borate), KTP (potassium titanyl phosphate), LBO (lithium triborat) or LiNbO3 (lithium niobate) crystals.

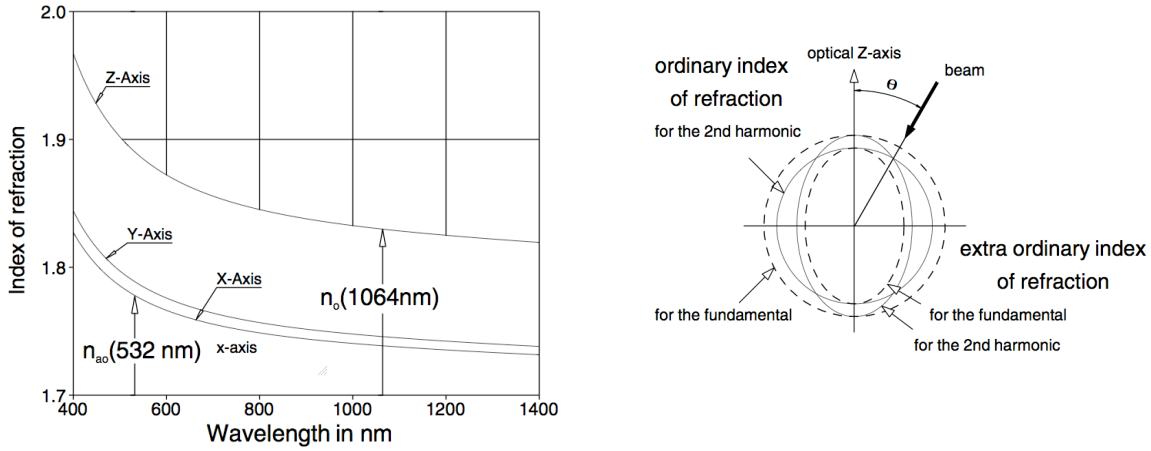

Fig. 4: Dispersion curve for the fundamental and second harmonic of the Nd:YAG laser in KTP (left). Schematic representation of a refractive index ellipsoid for achieving phase-matching in second harmonic generation within a birefringent, nonlinear crystal (right). Taken from [5].

3. Tasks

a) Continuous wave operation of the Nd:YAG laser (*review from Ba14*): Setup the basic components of the Nd:YAG laser given by the diode pump laser, telescope, Nd:YAG medium, and cavity mirrors. Calculate the optimal mirror distance for achieving the stability criterion assuming a hemispherical resonator with a flat end mirror coated on the back face of the active Nd:YAG medium and an output mirror of R = 100 mm. Bring the system into optimal lasing by adjusting the mirror angles, translation of the pump diode laser, distances of the telescope mirrors and the position of the medium for maximizing the laser power at 1064 nm using the photodiode and oscilloscope. Next, detect the Nd:YAG spatial mode with the CMOS chip and make fine adjustments to guarantee a TEM_{00} transversal mode by inserting the iris into the cavity as a spatial filter for limiting the angles of the modes. The iris should be adjusted to allow maximum Nd:YAG laser output power for the full range of the diode pump power settings. Once this is achieved, use the photodiode to record the output power of the Nd:YAG laser as a function of diode pump power. From the plot of the data, extract the threshold pump power for lasing as well as the slope efficiency of the Nd:YAG laser for resonant pumping of the 804.4 nm transition in the Nd:YAG medium (see *Appendix A* for the spectral calibration curve in the temperature settings of the diode pump laser). Further calculate the intracavity power assuming a transmission of 2% at 1064 nm for the output mirror in the range of 0 to 10 % losses. This data will be used for comparison to the efficiency of second harmonic operation at 532 nm. For all the measurements described above, the photodiode should generally be used to monitor changes in the Nd:YAG output power due to the sensitivity and resolution necessary for characterizing the transition into lasing. The voltage scale obtained with the photodiode can be calibrated to watts with a power meter that measures at the high power range of the diode and Nd:YAG laser.

Note1: The photodiode will saturate at high power levels giving a nonlinear response. Use neutral density filters to bring the measurements with the photodiode in the range below saturation. Do not use neutral filters for calibration with the power meter.

Note2: A low-pass edge filter should be used for blocking the residual pump laser emission before the detector for background free characterization of the 1064 nm emission.
Note3: The power in the emission of the pump diode must also be calibrated with the power meter in the range of the current settings above diode lasing in order to obtain the threshold pump power for the Nd:YAG laser as well as the slope efficiency and intracavity power.

b) Identifying different transversal modes of the Nd:YAG laser: Use the CMOS chip for detecting the output of the Nd:YAG laser and record images of the transversal modes. The pump power from the diode laser can be adjusted to obtain the best contrast for the images, which is generally achieved at higher power levels. By adjusting the angles of the output mirror, different TEM_{nm} can be generated as well as the superposition of multiple TEM_{nm}. Adjust the output mirror to obtain pure, clearly defined TEM_{nm} and convert the 8-bit gray scale (256 gray tones) of the bitmap files from the CMOS application into a 2-D numeric array. Analyze and identify at least three different transversal modes by numeric simulation using Laguerre-Gaussian or Hermite-Gaussian polynomials to fit cross-sections of the transversal modes.

Note1: A low-pass edge filter should be used for blocking the residual pump laser before the detector for background free characterization of the 1064 nm emission. Neutral density filters can also be used to avoid saturation of the CMOS chip.
Note2: A LabView application is available at the experiment for converting the 8-bit gray scale of the bitmap files from the CMOS detector software and analyzing cross-sections and areas.

c) Operating the Nd:YAG in a continuous wave, intracavity second harmonic mode: Insert the KTP crystal into the cavity and replace the mirror for the output coupler for fully reflecting 1064 nm and maximal transmission of 532 nm. Optimize the cavity mirrors and angles of the KTP crystal for the highest power at 532 nm emission. Measure the efficiency of the 532 nm output as a function of the diode laser pump power for pumping the 804.4 nm absorption band in the Nd:YAG medium (see the spectral calibration curve of the laser diode). Calculate the efficiency of the intracavity second harmonic generation using the intracavity power in 1064 nm for different power levels of the diode pump laser as well as the calibration of diode pump power from task (a). Assume that the output mirror for second harmonic mode transmits virtually all the radiation from the cavity at 532 nm ($T_{532} \simeq 100\%$) while containing near all the radiation at 1064 nm ($T_{1064} \simeq 0\%$). Perform the measurement for two different positions of the KTP crystal in the cavity – close to the Nd:YAG medium and close to the output mirror. Compare the efficiency of both positions in view of the change in the intracaviy intensity of the 1064 nm radiation close to and away from the focus of the output mirror. As performed under task (a), a power meter is used to calibrate the voltage scale of the photodiode to watts at high power levels of the radiation at 532 nm.

Note1: The photodiode will saturate at higher power levels giving a nonlinear response. Use neutral density filters to bring the measurements with the photodiode in the range below saturation.
Note2: A high-pass edge filter should be used for blocking the residual laser emission before the detector for background free characterization of the 532 nm emission.

d) Operating the Nd:YAG Laser in a Q-switched mode with intracavity second harmonic generation: Insert the Pockels cell into the cavity. Roughly adjust the components of the Nd:YAG laser to maximize the leakage from the laser cavity at 532 nm at the highest diode pump power level. Turn on the voltage supply to the Pockels cell and maximize the power of the 532 nm output by adjusting the voltage level as well as the cavity mirrors and the translation of the diode pump laser with the frequency generator off (continuous wave operation). Once the laser is running at maximum power, characterize the hold-off of the Pockels cell by plotting the power of the continuous wave 532 nm output as a function of the voltage level applied to the Pockels cell. Determine the contrast in the highest and lowest quality of the cavity and discuss the mechanism that allows for the Pockels cell to modulate the quality of the cavity (see *Appendix B* of the calibration of the voltage settings). Next, set the voltage of the Pockels cell to a value giving the highest output power of the frequency doubled Nd:YAG laser and turn on the frequency generator for pulsing the voltage to the Pockels cell at a frequency of 1-50 Hz. Characterize the pulse train emitted from the laser using the photodiode and oscilloscope. Use the T-piece for splitting the signal from the frequency generator and use one arm to trigger the oscilloscope. Determine the precise repetition rate of the pulse train with the trace recorded on the oscilloscope. Characterize the form of a single pulse with the oscilloscope and approximate the rise time, fall time and pulse duration at full-width half-maximum (FWHM). Using the power calibration from task (c) and the value of the precise repetition rate of the pulse train, calculate the pulse energy and pulse power of the laser emission for varying values in diode pump power. Compare the pulse power and time-averaged power of the pulse train in the Q-switched mode with the continuous wave power of the 532 nm emission from task (c).

Note1: The photodiode will saturate at higher power levels giving a nonlinear response. Use neutral density filters to bring the measurements with the photodiode in the range below saturation.
Note2: A high-pass edge filter should be used for blocking the residual laser emission before the detector for background free characterization of the 532 nm emission.

4. Experimental Setup

4.1 Schematic

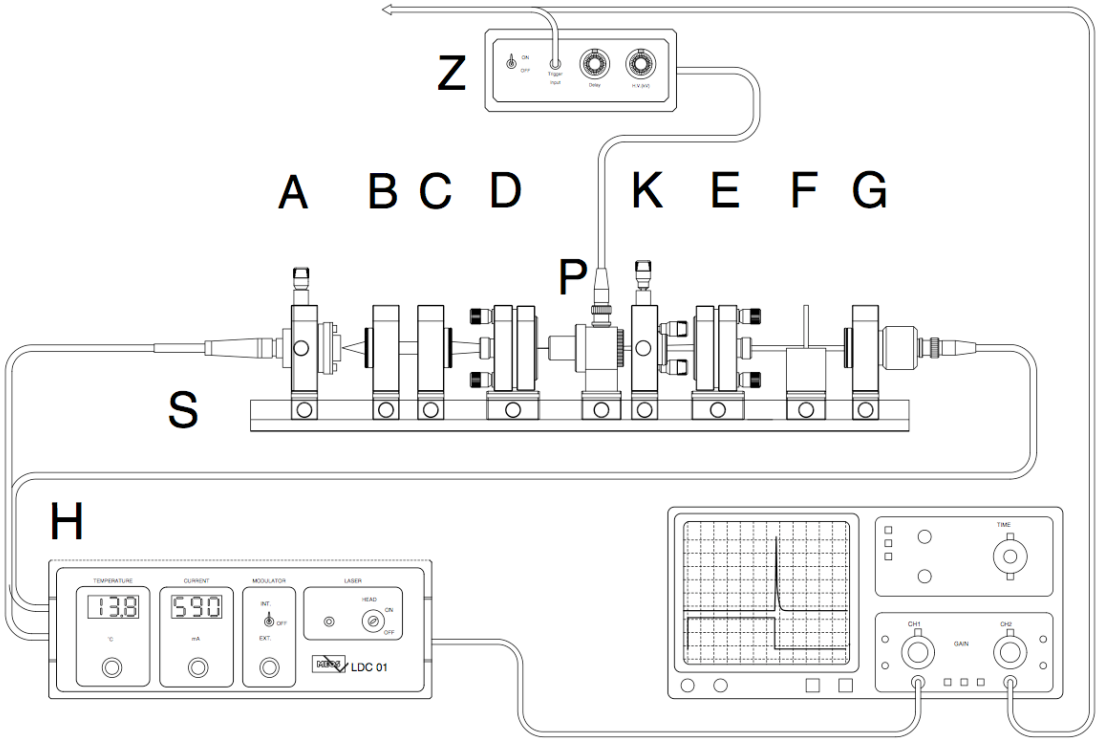

Fig. 5: Experimental setup for a Q-switched Nd:YAG laser with intracavity second harmonic generation.

4.2 Equipment List

	Device	**Note to the function**
A	diode pump laser	with current and temperature controller (**H**)
B	telescope lens	collimator for the laser diode emission
C	telescope lens	focusing of the laser diode emission
D	end mirror/Nd:YAG medium	coated for 532 and 1064 nm operation
E	output coupler	with mirrors for 532 and 1064 nm operation
F	filter holder	for high/low pass and gray filters + CMOS chip
G	photodiode	relative measurements of the laser output power
K	second harmonic unit	KTP crystal in a mount for angle adjustments
P	Pockels cell	Q-switch with high-voltage supply (**Z**)
O	oscilloscope	readout of the photodiode
S	slide rail	for optical mounts at variable distances

4.3 Notes on Certain Procedures

The operation manual of the Nd:YAG laser can be used for specific parameters and settings required for realizing tasks (a) - (d), which is also available in digital form at the experiment [5]. The tasks are designed so that points (a) and (c) are generally carried out and a choice or combination of conducting points (b) and (d) can be made. Each group should consult the tutor one week before the experiment concern how the tasks are emphasized. Also, the rules and procedures for safe and correct working with lasers should be thoroughly reviewed before conducting the experiment.

5. Notes on the Preparation, Analysis and Discussion

For the general and written preparation before the experiment, the subjects given in bold face in the text of Section 2 should be used as a list of key words relevant to the experiment. In the report, the analysis should be made using the values and plots that are obtained from tasks (a) – (d) in the experiment, whereby the relationship between different laser parameters should be emphasized as well as the comparison for different operational modes. In the discussion, the tendencies and relationships derived in the analysis of experimental data should be evaluated within the theoretical framework of the subjects given by the key words in bold face from Section 2.

6. Literature

[1] W. T. Silfvast, *Laser Fundamentals*, 2nd Edition, Cambridge University Press, Cambridge, 2004.
[2] E. Hecht, *Optics*, 4th Edition, Addison Wesley, San Francisco, 2002.
[3] R. Paschotta, *Encyclopedia of Laser Physics and Technology*, Wiley-VCH, Weinheim, 2008. (open access: http://www.rp-photonics.com/encyclopedia.html)
[4] J. Eichler, H.J. Eichler, *Laser: Bauformen, Strahlführung und Anwendungen*, 3rd Edition, Springer, Berlin, 2003.
[5] R. W. Boyd, *Nonlinear Optics*, 2nd Edition, Academic Press, San Diego, 1995.
[6] K. Dickmann, *Diode laser pumped Nd:YAG Laser*, (operation manual to the Nd:YAG Laser and advanced laboratory experiments), MEOS Cooperation.

Appendix A

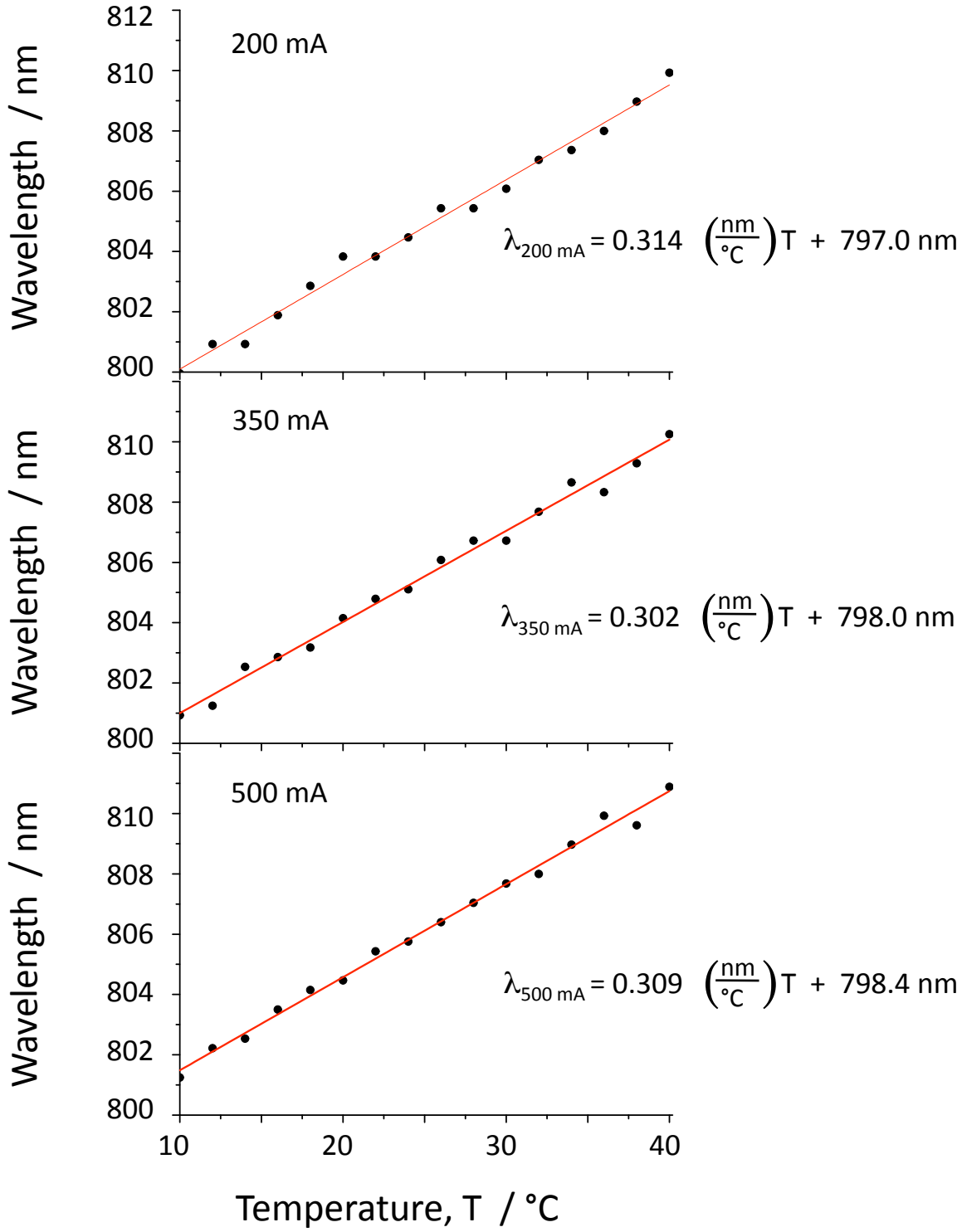
200 mA
350 mA
500 mA
Wavelength / nm
Temperature, T / °C
812
810
808
806
804
802
800
10
20
30
40
$\lambda_{200\ mA} = 0.314 \left(\frac{nm}{°C}\right) T + 797.0\ nm$
$\lambda_{350\ mA} = 0.302 \left(\frac{nm}{°C}\right) T + 798.0\ nm$
$\lambda_{500\ mA} = 0.309 \left(\frac{nm}{°C}\right) T + 798.4\ nm$

Appendix B [6]

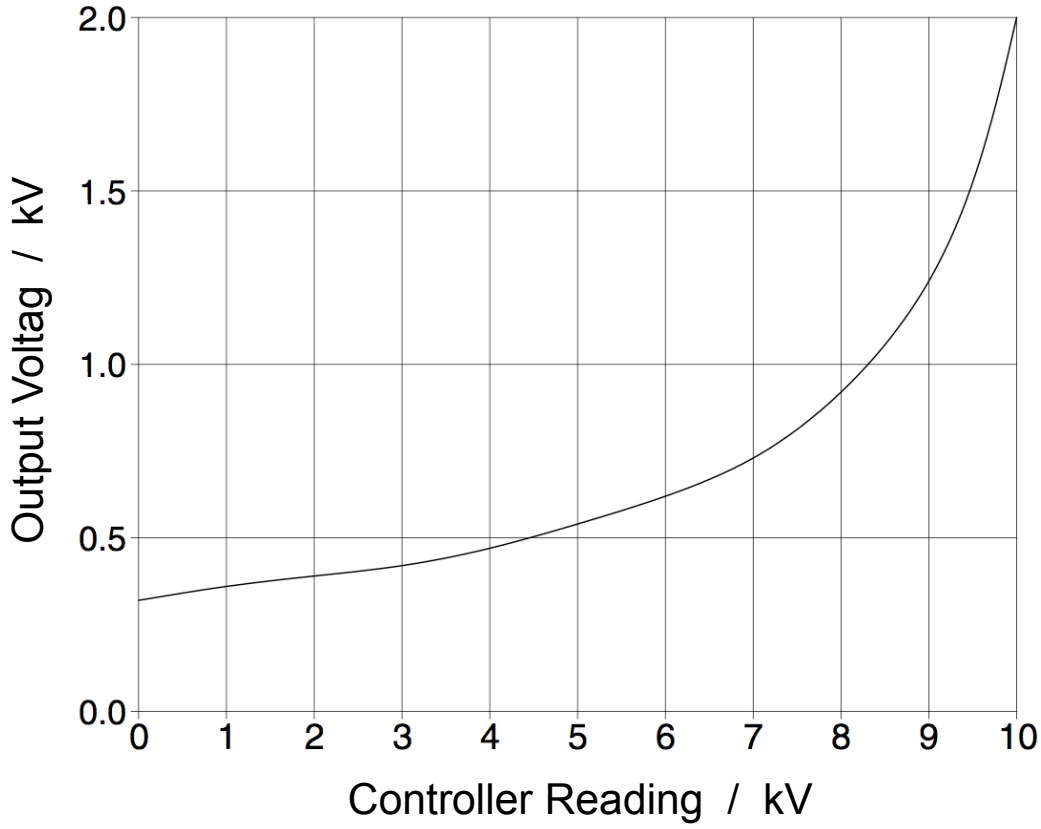
2.0
1.5
1.0
0.5
0.0
Output Voltag / kV
0
1
2
3
4
5
6
7
8
9
10
Controller Reading / kV